Bayesian Cramér-Rao Bound for Parameter Estimation Based on Mixed-Resolution Data

Yaniv Mazor, Itai E. Berman, and Tirza Routtenberg, *Senior Member, IEEE*

***Abstract*—In this paper, we consider Bayesian parameter estimation in systems incorporating both analog and 1-bit quantized measurements. We develop a tractable form of the Bayesian Cramér-Rao Bound (BCRB) specifically tailored for the linear-Gaussian mixed-resolution scheme. We discuss the properties of the BCRB and explore its suitability to serve as a system design tool. To this end, we present the partially-numerical linear minimum-mean-squared-error (LMMSE) estimator for a general threshold. In our simulations, the BCRB is compared with the mean-squared-error (MSE) of the LMMSE estimator and the numerical minimum MSE (MMSE) estimator for channel estimation with mixed analog-to-digital converters. The results demonstrate that the BCRB is not a tight lower bound on the MSE of these estimators. Moreover, the mixed-resolution BCRB fails to accurately capture the non-monotonic behavior of the estimators' MSEs versus signal-to-noise-ratio (SNR) and their behavior regarding different resource allocations. Consequently, while the BCRB provides some valuable insights, it requires careful examination before being used as a tool for system design in these scenarios.**

***Index Terms*—Bayesian parameter estimation, Bayesian Cramér-Rao bound (BCRB), quantization, mixed-resolution data**

I. Introduction

Estimation of unknown parameters from quantized observations has various applications in fields such as sensor networks [1-4], target tracking [5], and radar [6, 7]. Measurement quantization provides many advantages, including the reduction of hardware complexity, power consumption, and communication bandwidth. However, signal quantization introduces nonlinear effects into the system, which poses new challenges for estimation relying on quantized observations [8, 9]. Many practical systems incorporate sensors with multiple quantization resolutions, such as massive multiple-input multiple-output (MIMO) sydtems [10-12]. Therefore, developing performance bounds for parameter estimation with mixed analog and quantized data is crucial for performance analysis and system design [13] in many applications.

Lower bounds on the non-Bayesian mean-squared-error (MSE) for the estimation of deterministic parameters from quantized observations have been developed for the linear Gaussian model [1, 14] and for an unknown distribution [4]. In [9], the non-Bayesian Cramér-Rao Bound (CRB) was developed for additive-controlled perturbation of the quantizer thresholds for M-level quantized observations. The mixed-resolution CRB was discussed in [15]. Bayesian MSE lower bounds for 1-bit quantized data with dithering were developed in [16, 17]. Similarly, the Bayesian CRB (BCRB) with quantized compressed sensing measurements was derived in [18], and an upper bound on the BCRB for the quantized setting was proposed in [19, 20]. Quantization schemes that maximize the Fisher information matrix (FIM) and minimize the CRB were developed in [21] and [22], respectively.

Performance bounds play a crucial role in system design and the optimization of schemes with quantized data. For example, in [9] it is shown that random dithering can significantly reduce the CRB. In [23], deterministic dithering is shown to be optimal in terms of minimizing the BCRB. The optimization of the dithering approach based on the CRB has been explored in [9]. However, these works do not guarantee the achievability of the bounds by practical estimators, which is a major limitation on their practical relevance. For example, [1] shows that there could be a significant gap between the CRB based on 1-bit quantization and the MSE of the clairvoyant estimator when the dynamic range of the unknown parameter is large compared to the additive observation noise variance. In addition, the Bayesian bounds were developed for purely quantized data or for specific problems, and there are no existing tractable bounds for the linear-Gaussian mixed-resolution architecture.

In this work, we consider the estimation of random parameters based on both 1-bit quantized and analog (unquantized) measurements. We develop a closed-form expression of the mixed-resolution BCRB, which avoids matrix inversion due to the structure of the system matrices and the white noise assumption. Then, we discuss the properties of the BCRB and some special cases. We present the partially numerical linear minimum-mean-squared-error (LMMSE) estimator for a general threshold. Finally, we show via simulations that while the BCRB provides some valuable insights, it cannot serve as a system design tool for setting the resource allocation.

II. Mixed-Resolution Measurement Model

We consider the problem of estimating a complex-valued random parameter vector, $\boldsymbol{\theta} \in \mathbb{C}^M$, based on mixed-resolution data. We assume that $\boldsymbol{\theta}$ has a standard complex Gaussian distribution, $\boldsymbol{\theta} \sim \mathcal{CN}(\mathbf{0}, \mathbf{I})$. The available data consist of the following analog, high-resolution measurements:

$$\mathbf{x}_a = \mathbf{H}\boldsymbol{\theta} + \mathbf{u}_a, \tag{1}$$

where $\mathbf{H} = \left[\mathbf{H}_1^T, \mathbf{H}_2^T, \ldots, \mathbf{H}_{n_a}^T\right]^T \in \mathcal{C}^{N_a \times M}$, in which

$$\mathbf{H}_i^H \mathbf{H}_i = \rho_a \mathbf{I}_M, \quad \forall i = 1, \ldots, n_a, \tag{2}$$

The authors are with the School of Electrical and Computer Engineering Ben-Gurion University of the Negev Beer-Sheva 84105, Israel, e-mail: {mazya,itaieliy}@post.bgu.ac.il, tirzar@bgu.ac.il. This work is supported by the Israel Science Foundation (ISF), Grant No. 1148/22.

$N_a = n_a M$, and $\rho_a > 0$ is known. If $i \neq j$, then $\mathbf{H}_i^H \mathbf{H}_j$ can take arbitrary values. In addition, the data includes the following quantized, low-resolution measurements:

$$\mathbf{x}_q = \mathcal{Q}\left(\mathbf{G}\boldsymbol{\theta} + \mathbf{u}_q - \boldsymbol{\tau}\right), \tag{3}$$

where $\mathbf{G} = \mathbf{1}_{n_q} \otimes \mathbf{G}_1 \in \mathcal{Q}^{N_q \times M}$, in which $N_q = n_q M$,

$$\mathbf{G}_1^H \mathbf{G}_1 = \rho_q \mathbf{I}_M, \tag{4}$$

and $\rho_q > 0$ is known. The operator $\mathcal{Q}(\cdot)$ is the 1-bit quantization operator applied elementwisely, where

$$Q(z) = \frac{1}{\sqrt{2}}(\text{sgn}(\text{Re}\{z\}) + j\text{sgn}(\text{Im}\{z\})), \ \forall z \in \mathbb{C},$$

and $\text{sgn}(\cdot)$ is the sign function. The model in (3) enables diverse threshold values given by $\boldsymbol{\tau} \in \mathbb{C}^{N_q}$. The additive noises, $\mathbf{u}_a$ and $\mathbf{u}_q$, are independent, zero-mean, complex Gaussian vectors, $\mathbf{u}_a \sim \mathcal{CN}(\mathbf{0}, \sigma_a^2 \mathbf{I}_{N_a})$ and $\mathbf{u}_q \sim \mathcal{CN}(\mathbf{0}, \sigma_q^2 \mathbf{I}_{N_q})$, where σ_a, σ_q are known. The noise and the unknown parameter vectors, $\mathbf{u}_a$, $\mathbf{u}_q$, and $\boldsymbol{\theta}$, are assumed to be mutually independent.

The analog measurement model in (1) can be interpreted in practice as a model of sufficiently high-resolution measurements such that the residual quantization noise is negligible [24]. The considered model is applicable in various spheres, such as scalar estimation in sensor networks [1, 9], channel estimation in MIMO communications [25-30], and a sequential-time dynamic linear model with different data resolutions [26].

The goal of this estimation problem is to use mixed-resolution measurements, $\mathbf{x} \triangleq [\mathbf{x}_a^T, \mathbf{x}_q^T]^T$, to estimate $\boldsymbol{\theta}$. The minimum MSE (MMSE) and LMMSE estimators, and their MSEs, do not possess closed-form analytical expressions in this case with a general threshold $\boldsymbol{\tau}$, since the conditional probability density function (PDF), $p(\boldsymbol{\theta}|\mathbf{x})$, is intractable in the presence of quantized measurements (see, e.g. [10, 29]). In this letter, we discuss the ability of the BCRB to provide an appropriate tool for performance analysis and system design.

III. Bayesian Cramér-Rao bound (BCRB)

The BCRB is a lower bound on the MSE for the estimation of random parameters (see, e.g. p. 72 in [31]):

$$\text{E}[(\hat{\boldsymbol{\theta}} - \boldsymbol{\theta})(\hat{\boldsymbol{\theta}} - \boldsymbol{\theta})^{\text{H}}] \succeq \text{BCRB} \triangleq \mathbf{J}^{-1}, \tag{5}$$

where $\mathbf{J}$ is the Bayesian Fisher information matrix (BFIM) and $\hat{\boldsymbol{\theta}}$ is an estimator of $\boldsymbol{\theta}$, based on the observation vector $\mathbf{x}$. The notation $\succeq$ is in the sense of positive semidefinite cones.

In the following theorem, we develop a closed-form expression of the BCRB for the considered model that does not involve matrix inversions. To this end, we denote

$$d_n(\boldsymbol{\theta}) \triangleq \frac{\phi^2(\zeta_n^R)}{\Phi(\zeta_n^R)\Phi(-\zeta_n^R)} + \frac{\phi^2(\zeta_n^I)}{\Phi(\zeta_n^I)\Phi(-\zeta_n^I)}, \tag{6}$$

$$\zeta_n^R \triangleq \frac{\sqrt{2}}{\sigma_q}\text{Re}\{\mathbf{g}_n^T\boldsymbol{\theta} - \tau_n\}, \quad \zeta_n^I \triangleq \frac{\sqrt{2}}{\sigma_q}\text{Im}\{\mathbf{g}_n^T\boldsymbol{\theta} - \tau_n\}, \tag{7}$$

where $\mathbf{g}_n \in \mathcal{C}^{M\times 1}$ is the nth row of $\mathbf{G}$ as a column vector, and $\phi(\cdot)$ and $\Phi(\cdot)$ denote the standard normal PDF and cumulative distribution function (CDF), respectively. The properties of the function $\frac{\phi^2(x)}{\Phi(x)\Phi(-x)}$ from (6) are discussed in [16].

Theorem 1: Under the linear Gaussian model described in Section II, the BCRB is given by

$$\text{BCRB} = \frac{\sigma_q^2\sigma_a^2}{\rho_q}\sum_{m=1}^{M}\frac{\mathbf{g}_m^*\mathbf{g}_m^T}{\rho_a n_a \sigma_q^2 + \sigma_a^2\sigma_q^2 + \frac{1}{2}\text{E}_{\boldsymbol{\theta}}[d_m(\boldsymbol{\theta})]\rho_q n_q \sigma_a^2}. \tag{8}$$

Proof: In order to derive the BCRB, we first validate that the associated regularity conditions [13] are satisfied for the considered scheme, as detailed in the supplemental material. Second, we use the fact that the BFIM satisfies [32, p. 173]

$$\mathbf{J} = \mathbf{J}_{\boldsymbol{\theta}} + \text{E}_{\boldsymbol{\theta}}[\mathbf{J}_{\mathbf{x}|\boldsymbol{\theta}}], \tag{9}$$

where the prior FIM for the Gaussian case is [31, p. 85]

$$\mathbf{J}_{\boldsymbol{\theta}} = \mathbf{I}_M, \tag{10}$$

and the posterior is defined as [32, p. 173]

$$\text{E}_{\boldsymbol{\theta}}[\mathbf{J}_{\mathbf{x}|\boldsymbol{\theta}}] = \text{E}_{\boldsymbol{\theta}}\left[\text{E}_{\mathbf{x}|\boldsymbol{\theta}}\left[\nabla_{\boldsymbol{\theta}}^H \log p(\mathbf{x}|\boldsymbol{\theta}) \nabla_{\boldsymbol{\theta}} \log p(\mathbf{x}|\boldsymbol{\theta})\right]\right], \tag{11}$$

where $\nabla_{\boldsymbol{\theta}}$ denotes the gradient with respect to (w.r.t.) $\boldsymbol{\theta}$. Since the analog and quantized observations are independent given $\boldsymbol{\theta}$, i.e. $\log p(\mathbf{x}|\boldsymbol{\theta}) = \log p(\mathbf{x}_a|\boldsymbol{\theta}) + \log p(\mathbf{x}_q|\boldsymbol{\theta})$[1], and both likelihoods satisfy the smoothness condition given $\boldsymbol{\theta}$ (see more in the supplemental material), then

$$\text{E}_{\boldsymbol{\theta}}[\mathbf{J}_{\mathbf{x}|\boldsymbol{\theta}}] = \text{E}_{\boldsymbol{\theta}}[\mathbf{J}_{\mathbf{x}_a|\boldsymbol{\theta}}] + \text{E}_{\boldsymbol{\theta}}[\mathbf{J}_{\mathbf{x}_q|\boldsymbol{\theta}}], \tag{12}$$

where the FIMs based on each set of measurements $\mathbf{x}_a$ and $\mathbf{x}_q$, respectively, given $\boldsymbol{\theta}$, are (see, e.g. [16, 33])

$$\mathbf{J}_{\mathbf{x}_a|\boldsymbol{\theta}} \triangleq \text{E}_{\mathbf{x}_a|\boldsymbol{\theta}}\left[\nabla_{\boldsymbol{\theta}}^H \log p(\mathbf{x}_a|\boldsymbol{\theta}) \nabla_{\boldsymbol{\theta}} \log p(\mathbf{x}_a|\boldsymbol{\theta})\right], \tag{13a}$$

$$\mathbf{J}_{\mathbf{x}_q|\boldsymbol{\theta}} \triangleq \text{E}_{\mathbf{x}_q|\boldsymbol{\theta}}\left[\nabla_{\boldsymbol{\theta}}^H \log p(\mathbf{x}_q|\boldsymbol{\theta}) \nabla_{\boldsymbol{\theta}} \log p(\mathbf{x}_q|\boldsymbol{\theta})\right]. \tag{13b}$$

Given $\boldsymbol{\theta}$, the analog measurements have a complex Gaussian distribution, and thus, the FIM from (13a) equals [33, pp. 529]

$$\mathbf{J}_{\mathbf{x}_a|\boldsymbol{\theta}} = \frac{1}{\sigma_a^2}\mathbf{H}^H\mathbf{H} = \frac{\rho_a n_a}{\sigma_a^2}\mathbf{I}_M, \tag{14}$$

where the last equality is obtained by substituting (2). In the supplemental material, it is shown that (13b) is reduced to

$$\mathbf{J}_{\mathbf{x}_q|\boldsymbol{\theta}} = \frac{1}{2\sigma_q^2}\mathbf{G}^H\mathbf{D}(\boldsymbol{\theta})\mathbf{G} = \frac{n_q}{2\sigma_q^2}\sum_{m=1}^{M} d_m(\boldsymbol{\theta})\mathbf{g}_m^*\mathbf{g}_m^T, \tag{15}$$

where $\mathbf{D}(\boldsymbol{\theta}) = \text{diag}\left([d_1(\boldsymbol{\theta}), \cdots, d_M(\boldsymbol{\theta})]\right)$ and the last equality holds since $\mathbf{G}$ is a block matrix. Overall, substituting (10), (12), (14), and (15) into (9) yields

$$\begin{aligned}\mathbf{J} &= \left(1 + \tfrac{\rho_a n_a}{\sigma_a^2}\right)\mathbf{I}_M + \tfrac{n_q}{2\sigma_q^2}\textstyle\sum_{m=1}^{M}\text{E}_{\boldsymbol{\theta}}[d_m(\boldsymbol{\theta})]\mathbf{g}_m^*\mathbf{g}_m^T \\ &= \tfrac{1}{\rho_q}\mathbf{G}_1^H\left(\tfrac{\sigma_a^2 + \rho_a n_a}{\sigma_a^2}\mathbf{I}_M + \tfrac{\rho_q n_q}{2\sigma_q^2}\mathbf{D}\right)\mathbf{G}_1,\end{aligned} \tag{16}$$

where $\mathbf{D} = \text{E}_{\boldsymbol{\theta}}[\mathbf{D}(\boldsymbol{\theta})]$. For a non-singular $\mathbf{D}$, (16) implies the BCRB in (8). ∎

It should be noted that $\text{E}_{\boldsymbol{\theta}}[d_m(\boldsymbol{\theta})]$ is analytically computed for $\tau = 0$, and is numerically evaluated for the general case. In addition, if $\mathbf{G}$ is not a block matrix, and (2) and (4) are not satisfied, then by substituting (10), (12), and the intermediate stages of (14) and (15) into (9) the BFIM in this case is

$$\mathbf{J} = \mathbf{I}_M + \frac{1}{\sigma_a^2}\mathbf{H}^H\mathbf{H} + \frac{1}{2\sigma_q^2}\mathbf{G}^H\mathbf{D}\mathbf{G}. \tag{17}$$

[1]For the sake of simplicity, we denote both PDF, probability mass function (PMF), and their mixed version by $p(\cdot)$.

IV. BCRB Properties

In this section, we discuss the single-resolution bounds in Subsection IV-A, and the effect of quantization on the mixed BCRB in Subsection IV-B.

A. Single resolution case

In this part, we show the BCRB from Theorem 1 for the two extreme cases of single-resolution data.

1) Analog measurements only: By substituting $n_q = 0$ in the first row of (16), we obtain that the BFIM in this case is given by $\mathbf{J} = \left(1 + \frac{\rho_a n_a}{\sigma_a^2}\right)\mathbf{I}_M$. The BCRB, easily calculated by the inverse of this BFIM, is given for this analog case by

$$\text{BCRB} = \frac{\sigma_a^2}{\rho_a n_a + \sigma_a^2}\mathbf{I}_M. \tag{18}$$

2) Quantized measurements only: Substituting $n_a = 0$ in (16), results in $\mathbf{J} = \frac{1}{\rho_q}\mathbf{G}_1^H\left(\mathbf{I}_M + \frac{\rho_q n_q}{2\sigma_q^2}\mathbf{D}\right)\mathbf{G}_1$. Accordingly, the BCRB (the inverse of the BFIM) is reduced to

$$\text{BCRB} = \frac{2\sigma_q^2}{\rho_q}\sum_{m=1}^{M}\frac{1}{2\sigma_q^2 + \rho_q n_q \mathrm{E}_{\boldsymbol{\theta}}[d_m(\boldsymbol{\theta})]}\mathbf{g}_m^*\mathbf{g}_m^T, \tag{19}$$

which is similar to existing 1-bit quantized BCRB results [34].

B. The effect of quantization on the mixed BCRB

In the following, we investigate the relations between the proposed mixed resolution BCRB, which is based on $\mathbf{x}_a$ and $\mathbf{x}_q$, and a pure analog BCRB, BCRB_{pa}, which is based on $\mathbf{x}_a$ and $\mathbf{G}\boldsymbol{\theta} + \mathbf{u}_q$ (see in (3)), i.e. without quantization, in order to analyze the effect of the quantization on the mixed BCRB. First, we note that similar to (18), it can be shown that

$$\text{BCRB}_{pa} = \mathbf{J}_{pa}^{-1} = \frac{\sigma_q^2\sigma_a^2}{\sigma_q^2\left(\rho_a n_a + \sigma_a^2\right) + \sigma_a^2\rho_q n_q}\mathbf{I}_M. \tag{20}$$

Claim 1: For non-singular BFIMs, we have

$$\text{BCRB}_{pa} \preceq \text{BCRB}. \tag{21}$$

Claim 1 is intuitively convincing, as the measurements prior to quantization inherently possess more information on $\boldsymbol{\theta}$, leading to a lower MSE and a reduced lower bound.

Proof: The inequality $\frac{\phi^2(x)}{\Phi(x)\Phi(-x)} \leq \frac{2}{\pi}$, $\forall x \in \mathbb{R}$ (see Eqs. (103)-(109) in [16]) implies that $d_n(\boldsymbol{\theta})$ from (6) satisfies

$$d_n(\boldsymbol{\theta}) \leq \frac{4}{\pi}, \quad \forall n = 1,\ldots,M, \quad \forall \boldsymbol{\theta} \in \mathbb{C}^M. \tag{22}$$

By using (16) and (20) and reorganizing, one obtains

$$\begin{aligned}\mathbf{J}_{pa} - \mathbf{J} &= \frac{\rho_q n_q}{\sigma_q^2}\mathbf{I}_M - \frac{n_q}{2\sigma_q^2}\mathbf{G}_1^H\mathbf{D}\mathbf{G}_1 \\ &= \frac{n_q}{\sigma_q^2}\mathbf{G}_1^H\left(\mathbf{I}_M - \frac{1}{2}\mathbf{D}\right)\mathbf{G}_1 \succeq \mathbf{0},\end{aligned} \tag{23}$$

where the second equality is obtained using the orthogonality in (4), and the last inequality is obtained since (22) implies that the diagonal matrix $\mathbf{I}_M - \frac{1}{2}\mathbf{D}$ has non-negative elements. Then, (23) implies that for non-singular BFIMs, $\mathbf{J}_{pa}$ and $\mathbf{J}$, the inequality in (21) holds. ∎

We now discuss the influence of quantization in the asymptotic regimes. Note that by using (16) and (20), one obtains

$$\begin{aligned}&\text{BCRB}^{-1} \times \text{BCRB}_{pa} = \mathbf{J} \times \mathbf{J}_{pa}^{-1} \\ &= \frac{\sigma_q^2\left(\rho_a n_a + \sigma_a^2\right)}{\rho_q n_q \sigma_a^2 + \rho_a n_a \sigma_q^2 + \sigma_q^2\sigma_a^2}\mathbf{I}_M \\ &+ \frac{\sigma_a^2 n_q}{2\left(\rho_q n_q \sigma_a^2 + \rho_a n_a \sigma_q^2 + \sigma_q^2\sigma_a^2\right)}\sum_{m=1}^{M}\mathrm{E}_{\boldsymbol{\theta}}[d_m(\boldsymbol{\theta})]\mathbf{g}_m^*\mathbf{g}_m^T.\end{aligned} \tag{24}$$

In the asymptotic case w.r.t. to the observations, i.e. for $n_q, n_a \to \infty$, (24) is reduced to

$$\begin{aligned}\lim_{n_q,n_a\to\infty}\text{BCRB}^{-1} \times \text{BCRB}_{pa} &= \frac{\sigma_q^2\rho_a}{\rho_q\sigma_a^2 + \rho_a\sigma_q^2}\mathbf{I}_M \\ &+ \frac{\sigma_a^2}{2(\rho_q\sigma_a^2 + \rho_a\sigma_q^2)}\sum_{m=1}^{M}\mathrm{E}_{\boldsymbol{\theta}}[d_m(\boldsymbol{\theta})]\mathbf{g}_m^*\mathbf{g}_m^T.\end{aligned} \tag{25}$$

In particular, for the scalar case ($M = 1$) with $\rho_a = \rho_1 = \sigma_a = \sigma_q = 1, \boldsymbol{\tau} = \mathbf{0}$ and a deterministic θ ($\sigma_\theta^2 \to 0$), the parameter $\mathrm{E}_{\boldsymbol{\theta}}[d_m(\boldsymbol{\theta})]$ (see (6)) approaches $\frac{4}{\pi}$, and we get

$$\lim_{n_q,n_a\to\infty}\frac{\mathbf{J}}{\mathbf{J}_{pa}} \to \frac{\pi+2}{2\pi}. \tag{26}$$

Similarly, for the purely quantized setting, by substituting $n_a = 0$ and $n_q \to \infty$ in (25) we get $\frac{2}{\pi}$. This result coincides with the asymptotic loss of $\frac{\pi}{2}$ for single-bit quantization compared to unquantized data, which was shown in [9, 16].

For the case where $\sigma_a = \sigma_q = \sigma$, it can be seen that as σ^2 increases, the term in (24) is reduced to

$$\begin{aligned}\lim_{\sigma^2\to 0}\text{BCRB}^{-1}\text{BCRB}_{pa} &= \lim_{\sigma^2\to 0}\frac{1}{2\left(\rho_q n_q + \rho_a n_a\right)} \\ &\times\left(n_q\sum\nolimits_{m=1}^{M}\mathrm{E}_{\boldsymbol{\theta}}[d_m(\boldsymbol{\theta})]\mathbf{g}_m^*\mathbf{g}_m^T + 2\rho_a n_a\mathbf{I}_M\right).\end{aligned} \tag{27}$$

Analysis of $\mathrm{E}_{\boldsymbol{\theta}}[d_m(\boldsymbol{\theta})]$ in (6) shows that for $\sigma^2 \to 0$, $\mathrm{E}_{\boldsymbol{\theta}}[d_m(\boldsymbol{\theta})] \to 0$. Thus, for a finite M, (27) is reduced to

$$\lim_{\sigma^2\to 0}\mathbf{J} \times \mathbf{J}_{pa}^{-1} = \frac{\rho_a n_a}{\rho_q n_q + \rho_a n_a}\mathbf{I}_M. \tag{28}$$

The r.h.s. of (26) and (28) is always lower (in the matrix inequality sense) than the identity matrix since high-resolution measurements provide more significant information about $\boldsymbol{\theta}$.

V. Partially-numeric LMMSE estimator

The LMMSE estimator was derived in [10, 26]. However, no analytical form of the LMMSE estimator exists for a non-zero threshold, $\boldsymbol{\tau}$. Here, we present the partially-numeric LMMSE estimator for a general threshold. Since in the considered model $\boldsymbol{\theta}$ has a zero mean, the analytical LMMSE estimator is

$$\hat{\boldsymbol{\theta}} = \mathbf{C}_{\boldsymbol{\theta}\mathbf{x}}\mathbf{C}_{\mathbf{x}}^{-1}(\mathbf{x} - \mathrm{E}[\mathbf{x}]), \tag{29}$$

where for the mixed-resolution case,

$$\mathbf{C}_{\mathbf{x}} = \begin{bmatrix}\mathbf{C}_{\mathbf{x}_a} & \mathbf{C}_{\mathbf{x}_a\mathbf{x}_q} \\ \mathbf{C}_{\mathbf{x}_q\mathbf{x}_a} & \mathbf{C}_{\mathbf{x}_q}\end{bmatrix}, \quad \mathbf{C}_{\boldsymbol{\theta}\mathbf{x}} = \begin{bmatrix}\mathbf{C}_{\boldsymbol{\theta}\mathbf{x}_a} & \mathbf{C}_{\boldsymbol{\theta}\mathbf{x}_q}\end{bmatrix}, \tag{30}$$

and $\mathrm{E}[\mathbf{x}] = [\mathrm{E}[\mathbf{x}_a]^T, \mathrm{E}[\mathbf{x}_q]^T]^T$. We use the notation of the auto- and cross-covariance matrices of complex-valued vectors $\mathbf{a}$ and $\mathbf{b}$ as $\mathbf{C}_{\mathbf{a}} \triangleq \mathbf{C}_{\mathbf{aa}}$ and $\mathbf{C}_{\mathbf{ab}} \triangleq \mathrm{E}[(\mathbf{a} - \mathrm{E}[\mathbf{a}])(\mathbf{b} - \mathrm{E}[\mathbf{b}])^H]$.

While the matrices $\mathbf{C}_{\mathbf{x}_a}$, $\mathbf{C}_{\mathbf{x}_a}^{-1}$, and $\mathbf{C}_{\boldsymbol{\theta}\mathbf{x}_a}$ can be calculated analytically [26], the matrices, $\mathbf{C}_{\mathbf{x}_q}$, $\mathbf{C}_{\mathbf{x}_a\mathbf{x}_q}$, and $\mathbf{C}_{\boldsymbol{\theta}\mathbf{x}_q}$ cannot be analytically computed for $\boldsymbol{\tau} \neq \mathbf{0}$. Nonetheless, since the model is fully characterized (see Section II), we can generate dataset $\mathcal{D} = \{\boldsymbol{\theta}^{(t)}, \mathbf{x}_a^{(t)}, \mathbf{x}_q^{(t)}\}_{t=1}^{N_t}$ of i.i.d. samples from this model. This data can be used to evaluate the associated sample covariance matrices (SCM). For any vectors $\mathbf{a}$ and $\mathbf{b}$ with known means and associated data $\{\mathbf{a}^{(t)}, \mathbf{b}^{(t)}\}_{t=1}^{N_t}$, the SCM is

$$\hat{\mathbf{C}}_{\mathbf{ab}} = \frac{1}{N_t} \sum_{t=1}^{N_t} (\mathbf{a}^{(t)} - \mathrm{E}[\mathbf{a}])(\mathbf{b}^{(t)} - \mathrm{E}[\mathbf{b}])^H. \tag{31}$$

In our case, the expected value of $\mathbf{x}_a$ is $\mathbf{H}\boldsymbol{\theta}$, and the expectation of $\mathbf{x}_q$ is discussed in the supplemental material. Thus, we compute $\mathbf{C}_{\mathbf{x}}^{-1}$ by using use block matrix inversion as follows:

$$\hat{\mathbf{C}}_{\mathbf{x}}^{-1} = \begin{bmatrix} \mathbf{C}_{\mathbf{x}_a}^{-1} + \mathbf{C}_{\mathbf{x}_a}^{-1}\hat{\mathbf{C}}_{\mathbf{x}_a\mathbf{x}_q}\hat{\boldsymbol{\Delta}}^{-1}\hat{\mathbf{C}}_{\mathbf{x}_q\mathbf{x}_a}\mathbf{C}_{\mathbf{x}_a}^{-1} & -\mathbf{C}_{\mathbf{x}_a}^{-1}\hat{\mathbf{C}}_{\mathbf{x}_a\mathbf{x}_q}\hat{\boldsymbol{\Delta}}^{-1} \\ -\hat{\boldsymbol{\Delta}}^{-1}\hat{\mathbf{C}}_{\mathbf{x}_q\mathbf{x}_a}\mathbf{C}_{\mathbf{x}_a}^{-1} & \hat{\boldsymbol{\Delta}}^{-1} \end{bmatrix}. \tag{32}$$

Therefore, we need to compute the inverses of $\mathbf{C}_{\mathbf{x}_a}$ (which is tractable) and of $\hat{\boldsymbol{\Delta}} \triangleq \hat{\mathbf{C}}_{\mathbf{x}_q} - \hat{\mathbf{C}}_{\mathbf{x}_q\mathbf{x}_a}\mathbf{C}_{\mathbf{x}_a}^{-1}\hat{\mathbf{C}}_{\mathbf{x}_a\mathbf{x}_q}$. To avoid numerical stability issues, we add the commonly-used diagonal loading [35] prior to inverting the estimated matrix $\hat{\boldsymbol{\Delta}}$.

Algorithm 1: Partially-numeric mixed-resolution LMMSE estimator

Input: Distribution of $\mathbf{x}_a, \mathbf{x}_q, \boldsymbol{\theta}$, and ϵ
Output: Partially-numeric LMMSE estimator $\hat{\boldsymbol{\theta}}$.
1: Generate data, $\{\mathbf{x}_a^{(t)}, \mathbf{x}_q^{(t)}, \boldsymbol{\theta}^{(t)}\}_{t=1}^{N_t}$, and compute $\hat{\mathbf{C}}_{\mathbf{x}_q\boldsymbol{\theta}}, \hat{\mathbf{C}}_{\mathbf{x}_q}$, and $\hat{\mathbf{C}}_{\mathbf{x}_q\mathbf{x}_a}$ by (31)
2: Compute $\hat{\boldsymbol{\Delta}} = \hat{\mathbf{C}}_{\mathbf{x}_q} - \hat{\mathbf{C}}_{\mathbf{x}_q\mathbf{x}_a}\mathbf{C}_{\mathbf{x}_a}^{-1}\hat{\mathbf{C}}_{\mathbf{x}_a\mathbf{x}_q}$
3: Apply diagonal loading: $\hat{\boldsymbol{\Delta}} = \hat{\boldsymbol{\Delta}} + \epsilon\mathbf{I}$
4: Calculate $\mathbf{C}_{\mathbf{x}}^{-1}$ using block matrix inversion in (32)
5: Compute $\hat{\boldsymbol{\theta}} = [\mathbf{C}_{\boldsymbol{\theta}\mathbf{x}_a}, \hat{\mathbf{C}}_{\boldsymbol{\theta}\mathbf{x}_q}] \times \hat{\mathbf{C}}_{\mathbf{x}}^{-1}(\mathbf{x} - \mathrm{E}[\mathbf{x}])$

VI. Simulations

In this section, we numerically evaluate the behavior of the BCRB from (8) and compare it with the MSE of: 1) the MMSE estimator, evaluated via numerical integration; and 2) the LMMSE estimator implemented as in [26] for $\boldsymbol{\tau} = \mathbf{0}$, and by Algorithm 1 otherwise, where ϵ is the standard deviation of the eigenvalues of $\hat{\boldsymbol{\Delta}}$, as in [35]. We use 1,000 Monte-Carlo simulations, and the parameters $\sigma_a^2 = \sigma_q^2 = \sigma^2$, $\rho_a = \rho_q = 1$, and $N_t = 1,000$, for a scalar parameter estimation, $M = 1$.

In Fig. 1a we present the MSE of the estimators and the BCRB versus signal-to-noise ratio (SNR) for different partitions of the measurements, i.e. different pairs of n_a and n_q, for $\boldsymbol{\tau} = \mathbf{0}$. It can be seen that the MSEs of both estimators are not monotonic decreasing functions of the SNR, while the BCRB monotonically decreases as the SNR decreases. In addition, for high SNRs, the estimators rely solely on the analog observations and, thus, coincide (and are also equal to the analog-data least squared estimator). The BCRB does not capture the region where the quantized data becomes non-informative. Moreover, it can be seen that for high SNRs, the partition of $(n_a, n_q) = (2, 40)$ (pink, dashed lines) attains a lower MSE by both estimators than those obtained by $(n_a, n_q) = (1, 100)$ (blue, dashed lines), since for high SNR, the estimators' performance is determined by n_a. In contrast, the BCRB is higher for the second partition (blue, solid line) than for the first partition (pink, solid line) for any SNR. Thus, the BCRB cannot be used for determining the operational SNR or the resource allocation.

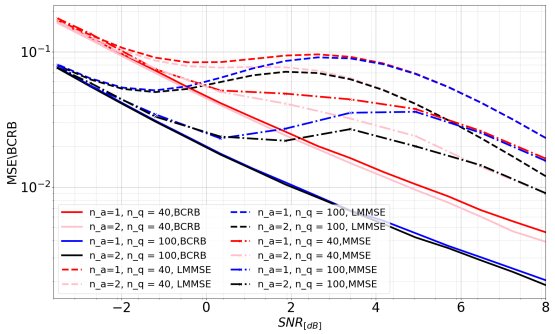

(a)

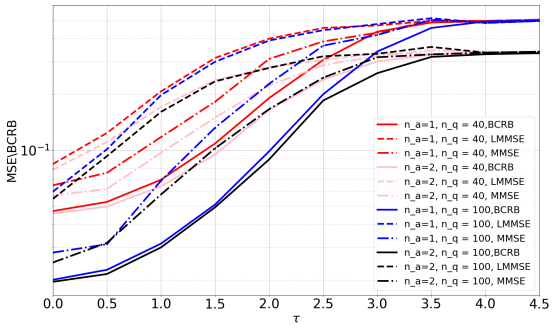

(b)

Fig. 1: The BCRB and MSE of the estimators (a) versus SNR for $\boldsymbol{\tau} = \mathbf{0}$; and (b) versus τ for SNR=0 dB.

Figure 1b illustrates how a constant threshold $\boldsymbol{\tau} = \tau\mathbf{1}$ affects the results. It can be seen that in the considered setting $\mathbf{g}_n^T\mathrm{E}[\boldsymbol{\theta}] = 0$ is the optimal value of τ for the bound and the estimators. As we approach $\tau = 0$, the bounds and estimators' MSE decrease. For large values of τ, both estimators converge to the BCRB, as the quantized information becomes negligible. However, in the intermediate region, $\tau \in [1.75, 2.75]$, the bounds do not accurately reflect the behavior of the estimators w.r.t. the resource allocation policy.

VII. Conclusions

In this paper, we consider mixed-resolution Bayesian estimation based on quantized and unquantized (analog) data, and we develop the BCRB for this setting. We analyze the properties of the mixed-resolution BCRB, compare it with the pure analog BCRB, and examine its asymptotic behavior. Additionally, we describe an algorithm to implement the partially numeric LMMSE estimator for a general threshold. Simulation results show that the BCRB for mixed-resolution data is unachievable by the MMSE and the LMMSE estimators outside the low SNR region, does not capture the non-monotonic behavior of the MSE versus SNR, and, hence, is not a suitable tool for optimizing the resource allocation. Future research should address tighter, large-error bounds for realistic performance analysis and effective system design.

REFERENCES

[1] A. Ribeiro and G. B. Giannakis, "Bandwidth-constrained distributed estimation for wireless sensor networks-part I: Gaussian case," *IEEE Trans. on signal processing*, vol. 54, no. 3, pp. 1131–1143, 2006.

[2] Y. Soydan and C. Candan, "A feedback quantization scheme leveraging fairness and throughput for heterogeneous multi-user diversity systems," *IEEE Transactions on Vehicular Technology*, vol. 59, no. 5, pp. 2610–2614, 2010.

[3] L. Xu, F. Gao, T. Zhou, S. Ma, and W. Zhang, "Joint channel estimation and mixed-ADCs allocation for massive MIMO via deep learning," *IEEE Trans. Wireless Communications*, vol. 22, no. 2, pp. 1029–1043, 2022.

[4] A. Ribeiro and G. Giannakis, "Bandwidth-constrained distributed estimation for wireless sensor networks-part II: Unknown probability density function," *IEEE Trans. on Signal Processing*, vol. 54, no. 7, pp. 2784–2796, 2006.

[5] A. Ribeiro, I. D. Schizas, S. I. Roumeliotis, and G. Giannakis, "Kalman filtering in wireless sensor networks," *IEEE Control Systems*, vol. 30, no. 2, pp. 66–86, 2010.

[6] M. Yeddanapudi, Y. Bar-Shalom, and K. Pattipati, "IMM estimation for multitarget-multisensor air traffic surveillance," *Proceedings of the IEEE*, vol. 85, no. 1, pp. 80–96, 1997.

[7] H. Chen, T. Kirubarajan, and Y. Bar-Shalom, "Tracking of spawning targets with multiple finite resolution sensors," *IEEE Transactions on Aerospace and Electronic Systems*, vol. 44, no. 1, 2008.

[8] M. S. Stein, S. Bar, J. A. Nossek, and J. Tabrikian, "Wireless channel estimation with low-complexity 1-bit ADC and unknown quantization threshold," *arXiv preprint arXiv:1703.02008*, 2017.

[9] H. C. Papadopoulos, G. W. Wornell, and A. V. Oppenheim, "Sequential signal encoding from noisy measurements using quantizers with dynamic bias control," *IEEE Trans. on Information Theory*, vol. 47, no. 3, pp. 978–1002, 2001.

[10] H. Pirzadeh and A. L. Swindlehurst, "Spectral efficiency of mixed-ADC massive MIMO," *IEEE Trans. Signal Processing*, vol. 66, no. 13, pp. 3599–3613, 2018.

[11] Y. Cheng, X. Shang, and F. Liu, "CRB analysis for mixed-ADC PMCW MIMO radar," in *2021 CIE International Conference on Radar (Radar)*, 2021, pp. 1032–1037.

[12] M. Waqeeb, T. S. Chowdhury, and Y. D. Zhang, "Cramér-Rao bound analysis of distributed DOA estimation exploiting mixed-precision covariance matrix," Apr. 2022.

[13] H. L. Van Trees and K. L. Bell, *"Bayesian Bounds for Parameter Estimation and Nonlinear Filtering/Tracking"*. Wiley-IEEE Press, 2007.

[14] J. Zhu, X. Lin, R. S. Blum, and Y. Gu, "Parameter estimation from quantized observations in multiplicative noise environments," *IEEE Trans. on Signal Processing*, vol. 63, no. 15, pp. 4037–4050, 2015.

[15] N. Harel and T. Routtenberg, "Non-Bayesian estimation with partially quantized observations," in *International Conference on Digital Signal Processing (DSP)*, 2017, pp. 1–5.

[16] G. Zeitler, G. Kramer, and A. C. Singer, "Bayesian parameter estimation using single-bit dithered quantization," *IEEE Trans. Signal Processing*, vol. 60, no. 6, pp. 2713–2726, 2012.

[17] S. Zeitz, F. Gast, M. Dorpinghaus, and G. Fettweis, "On the Bayesian Cramér-Rao bound for phase noise estimation based on 1-bit quantized samples," *IEEE Signal Process. Lett.*, Jan, 2023.

[18] S. S. Thoota and C. R. Murthy, "Massive MIMO-OFDM systems with low resolution ADCs: Cramér-Rao bound, sparse channel estimation, and soft symbol decoding," *IEEE Trans. Signal Processing*, vol. 70, pp. 4835–4850, 2022.

[19] Z. Shao, L. T. N. Landau, and R. C. de Lamare, "Channel estimation using 1-bit quantization and oversampling for large-scale multiple-antenna systems," in *IEEE International Conference on Acoustics, Speech and Signal Processing (ICASSP)*, 2019, pp. 4669–4673.

[20] M. Stein, S. Bar, J. Nossek, and J. Tabrikian, "Performance analysis for channel estimation with 1-bit ADC and unknown quantization threshold," vol. 66, no. 10, pp. 2557 – 2571, 2018.

[21] A. Vempaty, H. He, B. Chen, and P. K. Varshney, "On quantizer design for distributed Bayesian estimation in sensor networks," *IEEE Trans. Signal Processing*, vol. 62, no. 20, pp. 5359–5369, 2014.

[22] S. Kar, H. Chen, and P. K. Varshney, "Optimal identical binary quantizer design for distributed estimation," *IEEE Transa. Signal Processing*, vol. 60, no. 7, pp. 3896–3901, 2012.

[23] G. O. Balkan and S. Gezici, "CRLB based optimal noise enhanced parameter estimation using quantized observations," *IEEE Signal Processing Letters*, vol. 17, no. 5, pp. 477–480, 2010.

[24] N. Liang and W. Zhang, "Mixed-ADC massive MIMO," *IEEE Journal on Selected Areas in Communications*, vol. 34, no. 4, pp. 983–997, 2016.

[25] J. Park, S. Park, A. Yazdan, and R. W. Heath, "Optimization of mixed-ADC multi-antenna systems for cloud-RAN deployments," *IEEE Trans. Communications*, vol. 65, no. 9, pp. 3962–3975, 2017.

[26] I. E. Berman and T. Routtenberg, "Resource allocation and dithering of Bayesian parameter estimation using mixed-resolution data," *IEEE Trans. Signal Processing*, vol. 69, pp. 6148–6164, 2021.

[27] Y. Li, C. Tao, G. Seco-Granados, A. Mezghani, A. L. Swindlehurst, and L. Liu, "Channel estimation and performance analysis of one-bit massive MIMO systems," *IEEE Trans. Signal Processing*, vol. 65, no. 15, pp. 4075–4089, 2017.

[28] L. L. Geoffrey, Y. Li, A. L. Swindlehurst, A. Ashikhmin, and R. Zhang, "An overview of massive MIMO: Benefits and challenges," *IEEE Journal on Selected Topics in SignalProcessing*, 2014.

[29] Q. Wan, J. Fang, H. Duan, Z. Chen, and H. Li, "Generalized Bussgang LMMSE channel estimation for one-bit massive MIMO systems," *IEEE Trans. Wireless Communications*, vol. 19, no. 6, pp. 4234–4246, 2020.

[30] I.E. Berman and Tirza Routtenberg, "Partially linear bayesian estimation using mixed-resolution data," *IEEE SIGNAL PROCESSING LETTERS*, vol. 28, pp. 2202–2206, 2021.

[31] H. L. Van Trees, *"Detection, estimation, and modulation theory, part I: detection, estimation, and linear modulation theory"*. John Wiley & Sons, 2004.

[32] Peter J. Schreler, Louis L. Scharf, *"statistical signal processing of complex-valued data - the theory of improper and noncircular signals"*. Cambridge University Press, 2010.

[33] S. M. Kay, *"Fundamentals of Statistical Signal Processing: Estimation Theory"*. Prentice Hall, 1993.

[34] P. Stoica, X. Shang, and Y. Cheng, "The Cramér-Rao bound for signal parameter estimation from quantized data [lecture notes]," *IEEE Signal Processing Magazine*, vol. 39, no. 1, pp. 118–125, 2022.

[35] B. D. Carlson, "Covariance matrix estimation errors and diagonal loading in adaptive arrays," *IEEE Trans. Aerospace and Electronic Systems*, July 1988.